ARTHRITIS & RHEUMATISM
Vol. 54, No. 4, April 2006, pp 1198–1208
DOI 10.1002/art.21719

Targeting of Angiogenic Endothelial Cells at Sites of Inflammation by Dexamethasone Phosphate–Containing RGD Peptide Liposomes Inhibits Experimental Arthritis

Gerben A. Koning,[1] Raymond M. Schiffelers,[2] Marca H. M. Wauben,[2] Robbert J. Kok,[3] Enrico Mastrobattista,[2] Grietje Molema,[3] Timo L. M. ten Hagen,[4] and Gert Storm[2]

Objective. **To investigate whether RGD peptide–exposing long circulating polyethylene glycol (PEG) liposomes (RGD-PEG–L) targeted to $\alpha v\beta 3$ integrins expressed on angiogenic vascular endothelial cells (VECs) are able to bind VECs at sites of inflammation and whether such liposomes containing dexamethasone phosphate (DEXP) can be used as carriers to interfere with the development of experimental arthritis.**

Methods. **Binding and internalization of RGD-PEG–L were studied by fluorescence-activated cell sorting and confocal microscopy using fluorescently labeled liposomes. Radiolabeled liposomes were used to test in vivo pharmacokinetics and inflammation site targeting in lipopolysaccharide (LPS)–induced inflammation and adjuvant-induced arthritis (AIA) in rats. In vivo inflammation targeting was visualized by intravital microscopy using fluorescently labeled RGD-PEG–L. Therapeutic efficacy of DEXP-encapsulating RGD-PEG–L compared with nontargeted liposomes was evaluated in rats with AIA.**

Results. **RGD-PEG–L bound to and were taken up by proliferating human VECs in vitro. In vivo, increased targeting of radiolabeled RGD-PEG–L to areas of LPS-induced inflammation in rats was observed. Specific association with the blood vessel wall at the site of inflammation was confirmed by intravital microscopy. One single intravenous injection of DEXP encapsulated in RGD-PEG–L resulted in a strong and long-lasting antiarthritic effect in rat AIA.**

Conclusion. **RGD-targeted PEG liposomes represent an endothelial cell–specific drug delivery system that targets VECs at sites of inflammation. Use of these liposomes to deliver DEXP to VECs at arthritis-affected sites proved efficacious in rat adjuvant arthritis. These data indicate that VECs have an essential role in the inflammation process and suggest the possibility of using VEC targeting for therapeutic intervention in inflammatory processes such as arthritis.**

Vascular endothelial cells (VECs) play a crucial role in inflammation. They are involved in the recruitment of leukocytes into inflamed tissue and react to the demand of increased supply of oxygen and nutrients by formation of new blood vessels via the process of angiogenesis (1–3). The importance of angiogenesis in arthritic diseases, and of antiangiogenic treatment approaches, has recently gained considerable attention (4,5–7). In arthritis, both leukocyte recruitment and angiogenesis combined with the concomitant production of soluble inflammation mediators, such as growth factors and cytokines, by VECs allow for unwanted continuation and exacerbation of the inflammation. Specific targeting of VEC activity at inflamed sites therefore offers an attractive approach to study the role of VECs in inflammatory disease processes and may contribute to the development of new therapies.

VEC-specific targeting requires selective recog-

[1]Gerben A. Koning, PhD: Utrecht University, Utrecht, and Delft University of Technology, Delft, The Netherlands; [2]Raymond M. Schiffelers, PhD, Marca H. M. Wauben, PhD (current address: Leiden University Medical Center, Leiden, The Netherlands), Enrico Mastrobattista, PhD, Gert Storm, PhD: Utrecht University, Utrecht, The Netherlands; [3]Robbert J. Kok, PhD, Grietje Molema, PhD: University of Groningen, Groningen, The Netherlands; [4]Timo L. M. ten Hagen, PhD: Erasmus University Rotterdam, Rotterdam, The Netherlands.

Drs. Koning and Kok were members of UNYPHAR, a network collaboration between the Universities of Groningen, Leiden, and Utrecht and the pharmaceutical company Yamanouchi.

Address correspondence and reprint requests to Gert Storm, PhD, Department of Pharmaceutics, Utrecht Institute for Pharmaceutical Sciences, Utrecht University, PO Box 80082, 3508 TB Utrecht, The Netherlands. E-mail: g.storm@pharm.uu.nl.

Submitted for publication February 2, 2005; accepted in revised form December 19, 2005.

nition of this cell type at sites of inflammation by immunomodulatory agents. Cellular adhesion molecules or growth factor receptors that are preferentially expressed on VECs at inflamed sites may function as receptors for such recognition (1,3,8,9). The integrin $\alpha v\beta 3$ is strongly up-regulated on angiogenic endothelium at sites of inflammation (1,10,11). Arg-Gly-Asp (RGD) sequence–containing peptides with a cyclic conformation have been developed as specific ligands for $\alpha v\beta 3$ integrin (12).

Most reports on VEC-specific modulation as antiinflammatory therapy are limited to in vitro studies (9,13,14). To date only one report has described in vivo efficacy, in a study of a systemically applied dicyclic RGD peptide targeting a proapoptotic peptide directed to synovial neovasculature in murine collagen-induced arthritis (4).

Corticosteroids are known to be potent inflammation inhibitors that down-regulate the expression of cellular adhesion molecules, cytokines, and growth factors on endothelial cells (15–18) in an NF-κB–dependent manner (16,19), with decreased adhesion of immune cells as a consequence (20–22). Additionally, they exert significant antiangiogenic effects (23,24). Therefore, corticosteroids are potential compounds for use in VEC modulation. However, major disadvantages of the use of corticosteroids include their considerable systemic toxicity and short systemic half-life.

Encapsulation of corticosteroids in liposomes has been proven to reduce their side effects and increase their half-life and accumulation in the inflamed joint, resulting in strongly enhanced efficacy in rat adjuvant-induced arthritis (AIA) compared with administration of free corticosteroid (25–27). To direct the antiinflammatory activity to VECs at the site of inflammation, we encapsulated water-soluble dexamethasone phosphate (DEXP) in long-circulating, polyethylene glycol–coated liposomes (28) to which a cyclic RGD peptide was covalently attached (RGD-PEG–L). We selected an RGD peptide with high chemical stability and high affinity for $\alpha v\beta 3$ integrin, to target angiogenic VECs at sites of arthritis involvement (29,30). The peptide is equipped with a functional group that allows for covalent thioether linkage at the terminal end of the PEG chains on the surface of the long-circulating liposomes, thereby creating a multivalent RGD-exposing drug delivery system.

The aim of this study was to investigate whether targeted RGD-PEG–L containing DEXP are able to bind VECs at sites of inflammation and whether such liposomes can be used as a drug carrier to interfere with arthritis. We studied the interaction of RGD-PEG–L with VECs in vitro with regard to cell binding and internalization. Pharmacokinetics, biodistribution, and targeting potential of the RGD-PEG–L were assessed in healthy rats and in 3 animal models of inflammation, i.e., a rat AIA model and a lipopolysaccharide (LPS)–induced skin inflammation model in mice and rats. Finally the antiinflammatory activity of DEXP-containing RGD-PEG–L was studied in rat AIA.

MATERIALS AND METHODS

Materials. *N*-succinimidyl-S-acetylthioacetate and cholesterol were obtained from Sigma (St. Louis, MO). Dipalmitoylphosphatidylcholine (DPPC) was from Lipoid (Ludwigshafen, Germany). Maleimide–poly(ethylene glycol)$_{2000}$-distearoylphosphatidylethanolamine (Mal–PEG-DSPE) was obtained from Shearwater Polymers (Huntsville, AL). Methoxy–PEG-DSPE (mPEG-DSPE) and lissamine rhodamine B sulfonyl-diacyl-phosphatidylethanolamine (Rh-PE) were purchased from Avanti Polar Lipids (Alabaster, AL). ^{3}H-cholesteryloleylether (^{3}H-COE) was obtained from Amersham (Buckinghamshire, UK). Dexamethasone disodium phosphate was from Bufa (Uitgeest, The Netherlands). Sepharose CL-4B was from Pharmacia (Uppsala, Sweden). All chemicals were analytical grade or the best grade available.

Liposomes. Liposomes were composed of DPPC, cholesterol, mPEG-DSPE, and Mal–PEG-DSPE in a 1.85:1:0.075:0.075 molar ratio. When required, liposomes were labeled with trace amounts of ^{3}H-COE (0.25 Ci/mole total liposomal lipid [TL]) or with 0.1 mol% of the fluorescent bilayer marker Rh-PE or 1,1′-dioctadecyl-3,3,3′,3′-tetramethylindodicarbocyanine perchlorate (DiD; Molecular Probes, Leiden, The Netherlands). Lipids dissolved in chloroform and methanol were mixed, and a lipid film was made by rotary evaporation. The lipid film was hydrated in HN buffer (10 m*M* HEPES, 135 m*M* NaCl [pH 6.7]). DEXP was encapsulated by hydrating with HN buffer containing 50 mg/ml DEXP at a ratio of 1 mg DEXP/μmole total lipid. Liposomes were sized by repeated extrusion through polycarbonate membranes with a final pore size of 50 nm, using a high-pressure extruder (Lipex, Vancouver, British Columbia, Canada). Unencapsulated DEXP was separated from liposomal DEXP by gel permeation chromatography over a Sepharose CL-4B column, using HN buffer (pH 6.7) as eluent.

Liposomes for biodistribution studies using ^{67}Ga were formed in HN buffer containing 5 m*M* of the chelator deferoxamine mesylate (Desferal; Novartis, Basel, Switzerland). The ^{67}Ga was entrapped in preformed deferoxamine-containing liposomes as described previously (31).

Coupling of peptides to liposomes. The cyclic 5-mer RGD c(RGDf[ϵ-S-acetylthioacetyl])K and control RAD peptide c(RADf[ϵ-S-acetylthioacetyl])K (both described in ref. 30) were synthesized at a purity of 95% by Ansynth Service BV (Roosendaal, The Netherlands). The thioacetyl group was used for thioether linkage to the liposomes (32). Briefly, peptide was deacetylated in an aqueous solution of 0.05*M* HEPES/0.05*M* hydroxylamine HCl/0.03 m*M* EDTA (pH 7.0) for 30 minutes at room temperature. Next, the deprotected

peptide was incubated overnight at 4°C with the maleimide-containing liposomes at a ratio of 0.3, 1.0, or 3.0 μg peptide/μmole TL. Liposomes were purified by gel permeation chromatography over a Sepharose CL-4B column, using HN buffer (pH 7.4) as eluent. Alternatively, liposomes were separated from noncoupled peptides and concentrated by 2 ultracentrifugation steps of 75 minutes at 200,000*g* using a Beckman Optima LE-80K ultracentrifuge and a Ti70 fixed angle rotor, including rinsing with 10 ml of HN buffer (pH 7.4). Liposomes were stored under nitrogen at 4°C and used within 4 weeks after preparation.

Liposome characterization. Particle size and size distribution were determined by dynamic laser light scattering using a Malvern 4700 system (Malvern Instruments, Malvern, UK) equipped with a 75-mW argon laser (Uniphase, San Jose, CA). Data were analyzed with Automeasure software, version 3.2 (Malvern Instruments). The liposomes used in the present study had a mean particle size of 0.1 μm and a polydispersity of ~0.1; the latter is a measure of the variation in particle size and varies between 0 (monodispersed) and 1 (heterogeneous). The phospholipid phosphorus content of each liposome preparation was determined with a phosphate assay (33). DEXP-containing liposomes were extracted according to the method described by Bligh and Dyer (34), after which the organic phase was analyzed for phospholipid content. TL concentrations were calculated, taking into account the amount of liposomal cholesterol. DEXP content in the water/methanol phase was determined by reverse-phase high-performance liquid chromatography (RP-HPLC) over an Alltima RP18 column (Alltech, Breda, The Netherlands) with a mobile phase consisting of water (acidified to pH 2 with phosphoric acid)/acetonitrile (75:25 [volume/volume]). DEXP was detected by measuring the absorbance at 254 nm. Liposomal DEXP contents varied between 30 and 60 μg DEXP/μmole TL, representing an encapsulation efficiency of 3–6%.

The amount of RGD or RAD peptide coupled to the liposomes was detected indirectly by measuring the fraction of peptide not coupled to the liposomes obtained after separation of the liposomes. Peptide determination was done by RP-HPLC using a C-18 column (particle size 5 μm, length 250 mm; Alltima) with a gradient mobile phase changing within 30 minutes from 100% solvent A (acetonitrile:H_2O 5:95 [weight/weight]) to 25% solvent A and 75% solvent B (acetonitrile:H_2O 95:5 [w/w]). Solvent A and solvent B contained 0.08 volume % and 0.1 volume % trifluoroacetic acid, respectively. The peptide was detected by measuring the absorbance at 214 nm. In all peptide-liposome preparations, the detected amount of noncoupled peptide was <1% at the indicated peptide:liposome ratios. Similar results were obtained using a thiol and sulfide quantitation kit according to the instructions of the manufacturer (Molecular Probes). From these results it was calculated that at the peptide:lipid ratios of 0.3, 1.0, and 3.0 μg/μmole and the virtually quantitative coupling, ~30, 100, or 300 peptide molecules were coupled per liposome, assuming that 80,000 phospholipid molecules form 1 vesicle of 100 nm (35).

Cells. Human umbilical vein endothelial cells (HUVECs) were isolated according to the method of Jaffe et al (36) and cultured at 37°C in a 5% CO_2–containing humid atmosphere in RPMI 1640 medium containing 25 m*M* HEPES and 2 m*M* L-glutamine (Gibco, Breda, The Netherlands) supplemented with 20% (v/v) heat-inactivated fetal calf serum (Gibco), 100 IU/ml penicillin, 100 μg/ml streptomycin, and 0.25 μg/ml amphotericin B (Gibco). HUVECs were used up to passage 4. Cells growing in an 80% confluent monolayer were detached using 1 m*M* EDTA in phosphate buffered saline (PBS), after removal of the culture medium and repeated rinsing with PBS.

Fluorescence-activated cell sorter (FACS) analysis of liposome association with HUVECs. Detached cells (1×10^5) were transferred, in FACS buffer (PBS supplemented with 1% bovine serum albumin, $CaCl_2$ [1.26 m*M*], and $MgSO_4$ [0.81 m*M*]), to FACS tubes and incubated with various amounts of Rh-PE–labeled control PEG liposomes or RGD-PEG liposomes for 1 hour at 37°C or 4°C. The dependency of cell association on the liposomal peptide density was studied by adding 500 nmoles/ml liposomes with different RGD peptide densities. Next, cells were washed repeatedly in FACS buffer, fixed with 2% formaldehyde in PBS, and analyzed for fluorescence content with a flow cytometer (Becton Dickinson, Alphen ad Rijn, The Netherlands). Results were analyzed using WinMDI software, version 2.8 (Joseph Trotter, The Scripps Research Institute, La Jolla, CA). HUVECs expressed $\alpha v\beta 3$ integrin on their cell surface, as determined by FACS analysis using mouse monoclonal antibody BV3, specific for human $\alpha v\beta 3$ integrin (Abcam, Cambridge, UK).

Confocal laser scanning microscopy analysis of liposome uptake by HUVECs. HUVECs were plated in fibronectin-coated 16-well chamber slides and the next day were incubated for 1 hour with 200 nmoles TL/ml of DiD-labeled PEG-L, RAD-PEG–L, or RGD-PEG–L. After incubation, cells were washed 3 times with PBS (4°C) and fixed in 2% formaldehyde overnight at 4°C. After washing with PBS and deionized water, they were embedded in Fluorsave Reagent (Calbiochem, San Diego, CA) and covered with a glass coverslip. Images of cells were collected with a Leica TCS-SP confocal laser scanning microscope equipped with a 488-nm argon, 568-nm krypton, and 647-nm HeNe laser (Leica, Rijswijk, The Netherlands).

Animals. Female, specific pathogen–free RP/AEur/RijHsd strain albino rats (18–25 weeks of age, weighing 185–225 gm) (Harlan, Horst, The Netherlands) were used for induction of inflammation with LPS. Male BALB/c mice (6–8 weeks of age) were obtained from Charles River (Wilmington, MA) and used for window chamber studies.

For induction of AIA, male inbred Lewis rats between 7 and 9 weeks of age were obtained from the University of Limburg (Maastricht, The Netherlands). Rats were injected intradermally at the base of the tail with 0.1 ml of a 5 mg/ml suspension of heat-inactivated *Mycobacterium tuberculosis* in Freund's incomplete adjuvant (Difco, Detroit, MI). This results in the appearance of paw inflammation after ~10 days.

The animals were kept under conventional conditions and had access to standard pelleted chow and acidified water ad libitum. Experiments were performed according to national regulations, after approval by the local animal experiments ethical committee.

Liposome pharmacokinetics and biodistribution in rats with LPS-induced inflammation. LPS was administered subcutaneously (SC) to rats at a dose of 100 ng. Four hours later, rats were injected intravenously (IV) with ^{67}Ga-liposomes at 5 μmoles TL/kg. One, 4, 8, and 24 hours after liposome administration, blood samples were obtained by retroorbital bleeding using heparanized capillaries. Twenty-four hours after liposome administration, rats were killed and

inflamed skin samples, control skin samples, liver, spleen, lungs, and kidneys were dissected, weighed, and assessed for radioactivity content together with blood samples, using a Minaxi autogamma 5000 gamma counter (Packard, Meriden, CT). Blood clearance was represented as the percent of the injected dose. Blood volume was ~5.3% of the total body weight of the rat (31). For other tissues, the percent of the injected dose was represented per total organ or per gram of tissue, as indicated.

Visualization of vasculature binding of liposomes by intravital microscopy. The dorsal skinfold chamber was prepared by a modification of a procedure described by Papenfuss et al (37); we have previously described this modified procedure (38). Inflammation was induced in skin placed in the window chamber, by SC injection of 100 ng LPS in a volume of 10 μl. Four hours later, Rh-PE–labeled RGD-PEG–L or PEG-L was injected IV at a dose of 1 μmole. Mice were anesthetized by intraperitoneal administration of ketamine and xylazine and fixed to a microscope stage. The vasculature at the site of inflammation was viewed with a Leica DM-RXA fluorescence microscope. Images of the inflamed site were acquired using a Sony 3CCD DXC950 digital color video camera connected to a PC. Image acquisition and analysis were performed with Research Assistant 3.0 for Windows 98 (RVC, Hilversum, The Netherlands).

Liposome pharmacokinetics and biodistribution in rats with AIA. Pharmacokinetic and biodistribution studies were performed on arthritic rats (arthritis score of ≥8 [see below]; typically obtained on approximately day 20 after disease induction), by IV injection of ^{3}H-COE–labeled PEG-L or RGD-PEG–L at 5 μmole/kg. One, 2, 4, 8, and 24 hours after injection, with the rats under light anesthesia, blood samples from the tail were collected in EDTA-containing microtubes (Greiner, Alphen aan den Rijn, The Netherlands). Twenty-four hours after injection, rats were killed and the liver and spleen were dissected, weighed, and homogenized in PBS using a Potter Elvehjem tube (39). Blood samples and samples from liver and spleen homogenates were incubated for 1 hour at 50°C with Solvable (Packard, Groningen, The Netherlands) at a 1:2 ratio. All samples were discolored by incubation at 50°C with EDTA (0.1*M*) and hydrogen peroxide (30%) in a volume ratio of 1:0.5:1, until a pale yellow homogenate was obtained. Subsequently, samples were mixed with 10 ml Ultima Gold scintillation fluid (Packard) and, after overnight incubation, analyzed by scintillation measurement.

Treatment and clinical scoring of AIA. Rats were treated at disease onset, typically on day 11 or 12 after immunization, by a single IV injection of 1 mg/kg DEXP-encapsulating PEG liposomes or RGD liposomes, into the tail vein. Empty RGD liposomes at an equimolar dose were used as a control. Arthritis severity was scored by grading each paw from 0 to 4 based on erythema, swelling, and immobility of the joints, resulting in a maximum possible score of 16 per animal.

Statistical analysis. Statistical analysis was performed using GraphPad Prism 3.05 (GraphPad Software, San Diego, CA). The significance of differences in in vitro liposome cell association and in vivo targeting was evaluated by Student's 2-tailed unpaired *t*-test. For comparison of arthritis scores, the Mann-Whitney test was used.

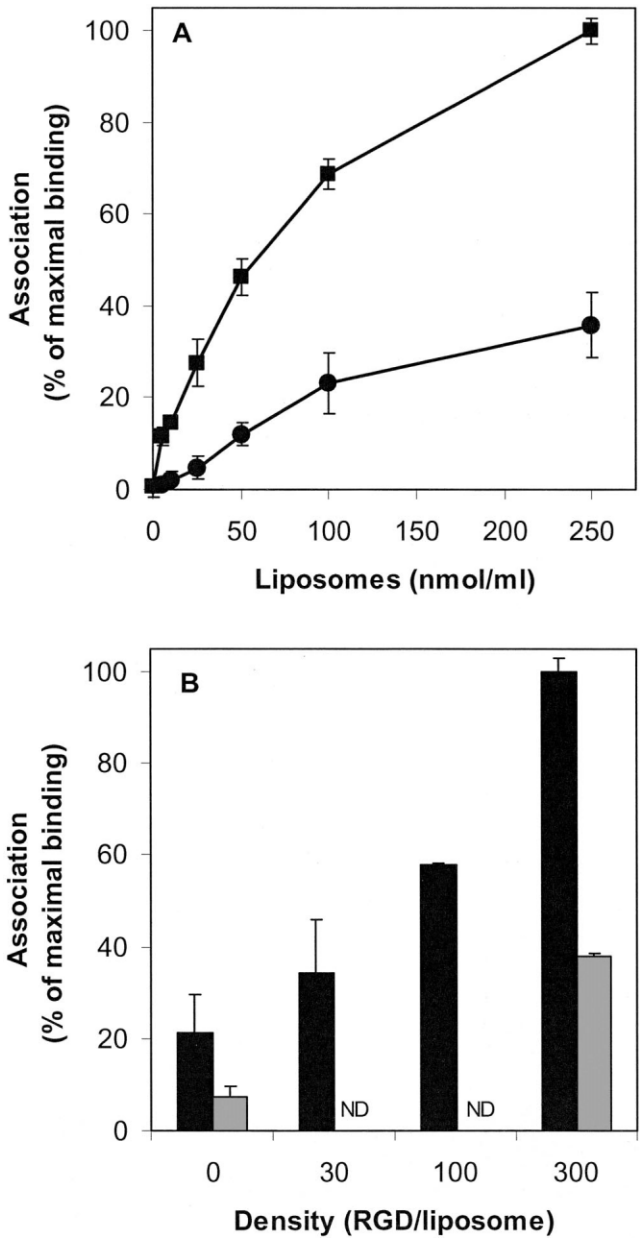

Figure 1. A, In vitro cell association of RGD peptide–exposing long-circulating polyethylene glycol liposomes (RGD-PEG–L) (■) and PEG-L (●) with human umbilical vein endothelial cells (HUVECs), as a function of liposome concentration. After incubation for 1 hour at 37°C with lissamine rhodamine B sulfonyl-diacyl-phosphatidyl-ethanolamine–containing liposomes and subsequent detachment of cells, fluorescence-activated cell sorter analysis was performed. RGD-PEG–L contained ~300 RGD peptide molecules per liposome. **B,** Increased association of RGD liposomes with HUVECs in vitro with increasing RGD density at the liposomal surface. A density of 100 or 300 RGD molecules per liposome resulted in a significant increase in association compared with liposomes without RGD (density 0) ($P <$ 0.005 by Student's unpaired *t*-test). Association was 3-fold lower at 4°C (shaded bars) than at 37°C (solid bars), indicating internalization of the liposomes. Values are the mean ± SEM from 4–5 separate experiments. ND = not determined.

RESULTS

Increased association of RGD-PEG liposomes with HUVECs. The cellular interaction of fluorescently labeled RGD-PEG–L with HUVECs was studied as a function of lipid concentration and liposomal peptide density during 1-hour incubation at 4°C and 37°C (Figure 1). The association of RGD-PEG–L with HUVECs, in comparison with control PEG-L (Figure 1A), was 6–10-fold higher at lipid concentrations of up to 25 nmoles/ml and 3–4-fold higher at concentrations >50 nmoles/ml, indicating saturable cell-specific association. The degree of association increased with an increase in RGD density from 0 to 300 molecules per liposome (Figure 1B). The degree of cell association showed a clear temperature dependency: the association of RGD-PEG–L with ~300 peptide molecules per liposome was approximately 3-fold lower at 4°C than at 37°C. This temperature-dependent association may represent the difference between cell binding at 4°C and cell binding combined with internalization occurring at 37°C.

Internalization of the RGD-PEG–L was evident from confocal laser scanning microscopy. Figure 2 shows a cell section, demonstrating intracellular punctate fluorescence. Significant levels of HUVEC-associated fluorescence were observed only upon incubation with RGD-PEG–L. Incubation with RAD-PEG–L or PEG-L without coupled peptide did not result in detectable levels of cell-associated fluorescence (results not shown). In addition, in a previous study we demonstrated the specificity of the in vitro interaction of RGD-PEG–L with HUVECs by showing strong inhibition of the RGD-PEG–L association with HUVECs by administration of excess amounts of free RGD peptide (38).

Enhanced targeting of RGD-PEG–L to sites of inflammation. In order to study the occurrence of VEC targeting to sites of inflammation, a rat model of LPS-induced inflammation was used. We quantified the amount of RGD-PEG–L localizing at the inflamed site in rats by using radioactively labeled liposomes administered 4 hours after induction of the inflammation. The degree of targeting, pharmacokinetics, and tissue distribution 24 hours after injection were also assessed. RGD-PEG–L, exposing 300 RGD molecules per particle, were more rapidly removed from the circulation than PEG-L without exposed RGD peptide (Figure 3A). The pharmacokinetics of PEG-L exposing 300 molecules of the control RAD peptide per liposome (RAD-PEG–L) was virtually identical to that of PEG-L without peptides, and thus strikingly different from that of RGD-PEG–L. Increased uptake of RGD-PEG–L in the liver, and even more increased uptake in the spleen (Figure 3B), compared with uptake of RAD-PEG–L and PEG-L was observed after 24 hours. RGD-PEG–L showed 3-fold increased targeting to the site of inflammation in comparison with RAD-PEG–L or PEG-L (Figure 3C). Levels of accumulation of RGD-PEG–L in inflamed skin were 6–10-fold higher than in normal skin.

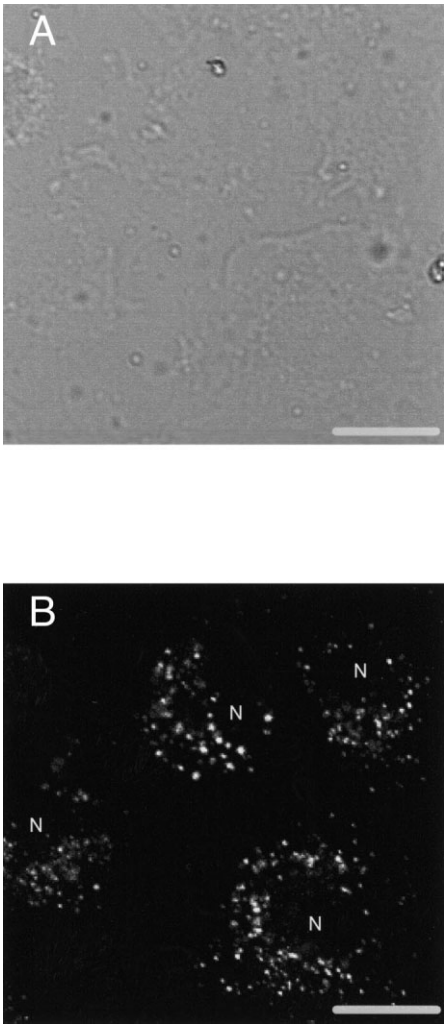

Figure 2. Internalization of fluorescently labeled RGD-PEG–L by HUVECs in vitro, as observed by confocal laser scanning microscopy. **A,** Transmitted light image. **B,** Fluorescent microscopic image of the same section as in **A**. Fluorescence appeared mainly perinuclear. **N** = nuclei. Bars = 20 μm. See Figure 1 for definitions.

Visualization of VEC binding at sites of inflammation. The binding of RGD-PEG–L to VECs at the inflamed site was examined in living animals by using

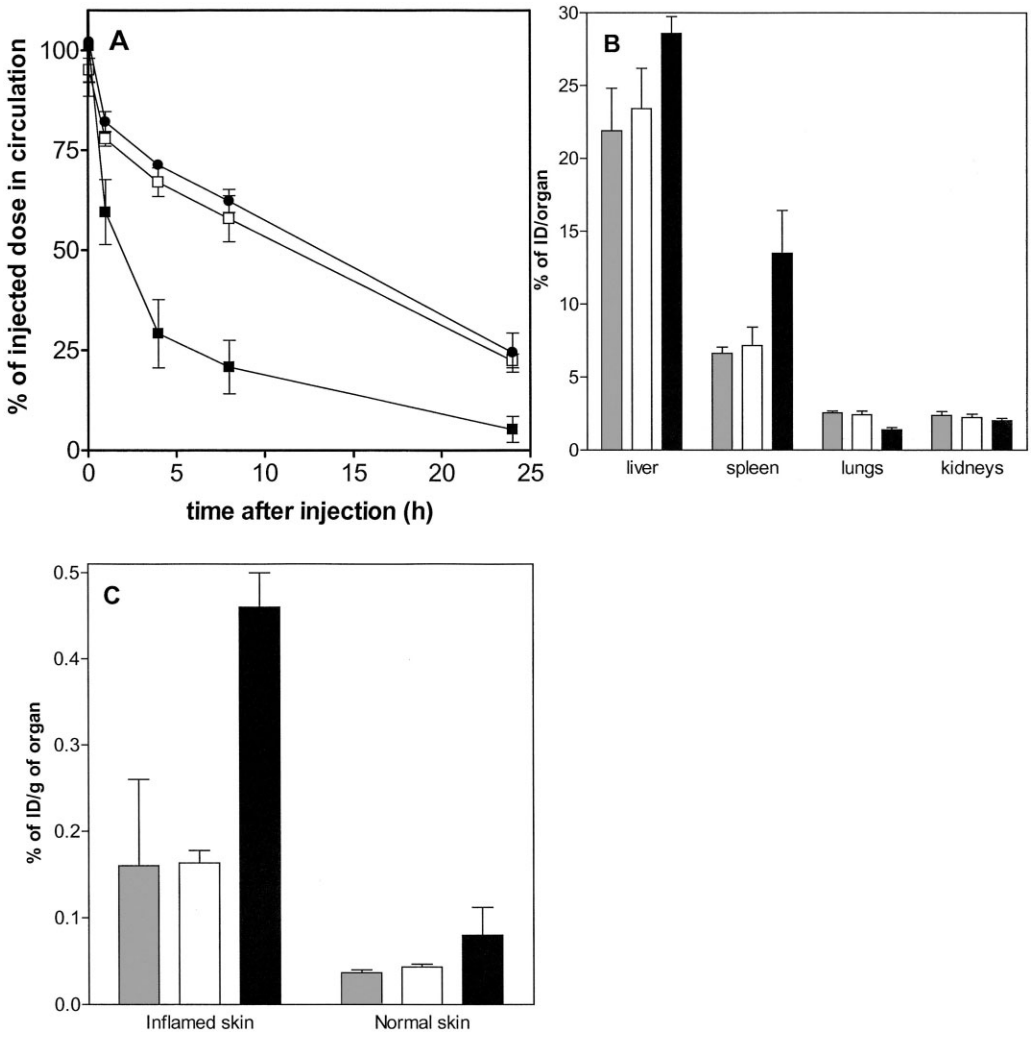

Figure 3. Pharmacokinetic behavior and target site localization of RGD peptide–exposing long-circulating polyethylene glycol liposomes (RGD-PEG–L), RAD-PEG–L, and PEG-L in rats with lipopolysaccharide-induced inflammation. Liposomes were administered intravenously (IV) 4 hours after induction of inflammation. **A,** Circulation kinetics during the 24 hours after injection of RGD-PEG–L (■), PEG-L (●), or RAD-PEG–L (□). **B** and **C,** Tissue distribution (**B**) and localization at site of inflammation (**C**) of RGD-PEG–L (solid bars), PEG-L (shaded bars), and RAD-PEG–L (open bars), determined 4 hours after IV administration. Circulation time of RGD-PEG–L was decreased compared with control RAD-PEG–L or PEG-L. The reduced circulation capacity could be explained by increased uptake in the liver and spleen. Strongly increased localization of RGD-PEG–L at the site of inflammation was observed in comparison with control liposomes ($P < 0.01$) and with localization in normal uninflamed skin ($P < 0.0001$). Values are the mean ± SD (n = 3–6 rats per group). ID = injected dose.

intravital microscopy with a dorsal flap window chamber, on a mouse in which inflammation had been induced by local SC administration of LPS. RGD-PEG–L injected 4 hours after induction of inflammation bound rapidly (within 1 hour) and extensively to the vessel wall at the inflamed site, in contrast to PEG-L (Figure 4). Binding of the RGD-PEG–L to the vessel wall was limited to the LPS-injected area, indicating specific targeting of these liposomes to VECs at inflamed vessels.

Increased clearance of RGD-PEG–L from the circulation in arthritic rats. The pharmacokinetic behavior of RGD-PEG–L with 300 RGD molecules per liposome, after IV injection into arthritic rats, was compared with that of PEG-L (Figure 5). Rats with an

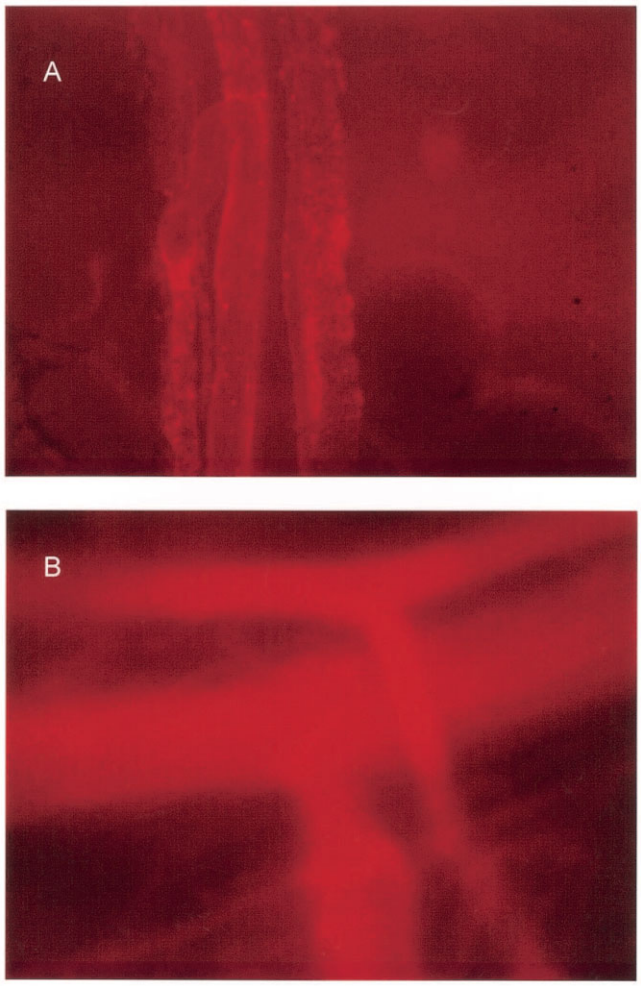

Figure 4. Intravital fluorescence microscopic images obtained from skin of a mouse with subcutaneous lipopolysaccharide (LPS)–induced inflammation, in a dorsal flap window chamber, demonstrating binding of fluorescently labeled RGD peptide–exposing long-circulating polyethylene glycol liposomes (RGD-PEG–L) (**A**), but not PEG-L (**B**), to the blood vessel wall at the inflamed site. Liposomes were injected intravenously 4 hours after LPS injection. Images were obtained 1 hour after injection of liposomes.

arthritis score of ≥8 were injected with ^{3}H-COE–labeled liposomes at a dose of 5 μmoles TL/kg body weight. Increased initial clearance, especially during the first 2 hours after injection, was observed with RGD-PEG–L in comparison with PEG-L (Figure 5A) and was accompanied by increased uptake in the liver, as observed 24 hours after injection (Figure 5B). Uptake of RGD-PEG–L in the spleen at 24 hours after injection was somewhat lower than uptake of PEG-L.

Enhanced therapeutic efficacy of DEXP-containing RGD-PEG liposomes in AIA. The antiarthritic activity of IV-administered DEXP-containing RGD-PEG liposomes (RGD-DEXP-PEG–L) was studied in comparison with that of DEXP-containing PEG liposomes (DEXP-PEG–L) and RGD-PEG–L without

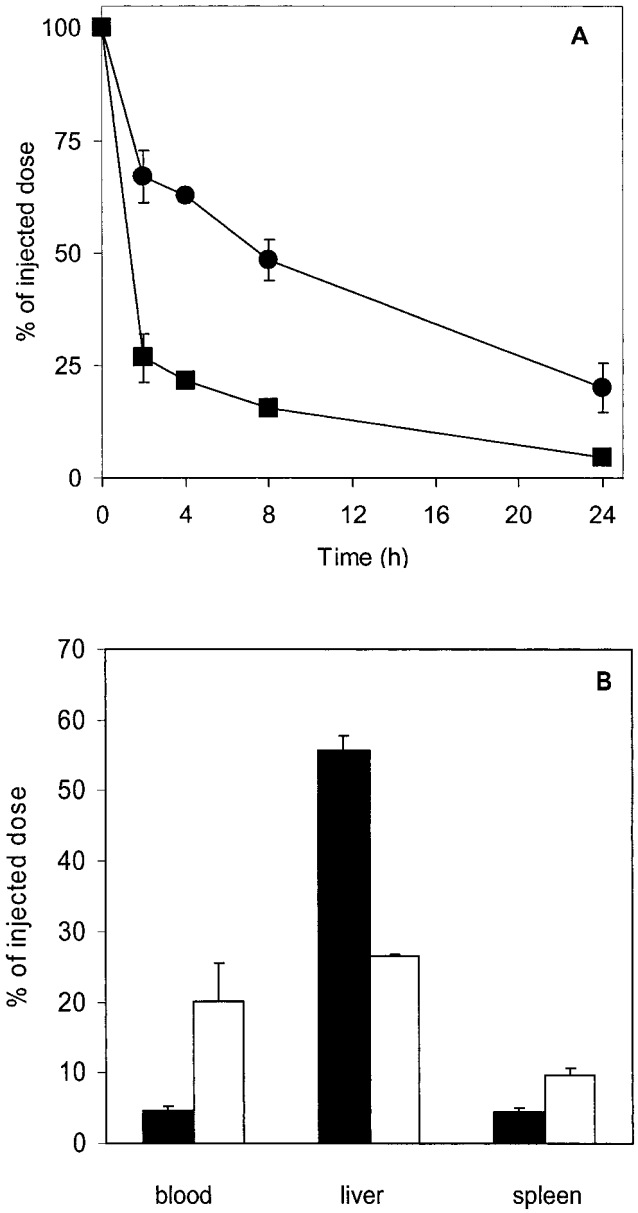

Figure 5. Pharmacokinetic behavior of RGD peptide–exposing long-circulating polyethylene glycol liposomes (RGD-PEG–L) and PEG-L in arthritic rats. Rats were inoculated with *Mycobacterium tuberculosis* in Freund's incomplete adjuvant to induce arthritis. Rats with ongoing arthritis (disease score ≥8) were injected intravenously with ^{3}H-cholesteryloleylether–labeled liposomes (5 μmoles total liposomal lipid/kg body weight). **A,** Increased clearance of RGD-PEG–L (■) from the circulation, compared with PEG-L (●) ($P < 0.03$). **B,** Increased uptake of RGD-PEG–L (solid bars) in the liver ($P = 0.0001$), compared with PEG-L (open bars).Values are the mean ± SD (n = 3 rats per group).

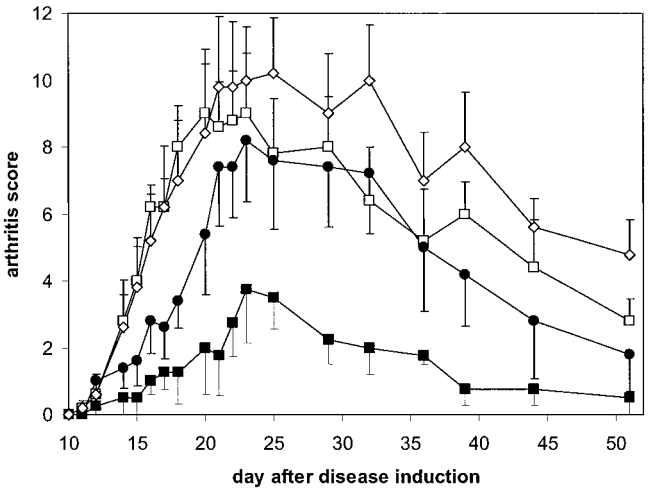

Figure 6. Therapeutic activity of systemically administered RGD-targeted dexamethasone phosphate (DEXP)–containing liposomes (■) in comparison with nontargeted DEXP liposomes (●), non–drug-containing RGD liposomes (□), and buffer-treated control (◇) in rats with adjuvant-induced arthritis. Rats were treated on day 12 by a single intravenous administration of one of the targeted or nontargeted liposomal DEXP preparations at 1 mg/kg, or with empty liposomes or buffer as controls. Values are the mean and SEM (n = 5 rats per group).

incorporated drug and buffer. Induction of adjuvant arthritis by immunizing rats with heat-inactivated *Mycobacterium tuberculosis* resulted in onset of the disease on day 12 after immunization. Rats were treated on this day by a single IV administration of 1 mg/kg DEXP in the various liposome formulations, or with an equimolar lipid dose for control formulations without DEXP (Figure 6). Treatment with RGD-DEXP-PEG–L strongly inhibited disease development during the first 3 days after treatment and also strongly reduced the peak levels of arthritis severity during the entire course of the disease. RGD-DEXP-PEG–L were by far more efficacious than either non–RGD-targeted DEXP-PEG–L or empty RGD-PEG–L treatments (both $P < 0.05$).

DISCUSSION

In this study we demonstrated that liposomes with coupled RGD peptides on their surface can be targeted to $\alpha v\beta 3$ integrins expressed on VECs. Targeting to human VECs was clearly observed in vitro and, more importantly, in vivo (to VECs at sites of inflammation in a model of SC LPS–induced inflammation in mice and rats). Loading such liposomes with the water-soluble corticosteroid DEXP, with the aim of interfering with VECs at areas of arthritis involvement, resulted in a strong and long-lasting antiarthritic effect with only a single IV injection in rats with AIA. Although the exact mechanism by which the RGD-DEXP-PEG liposomes are able to exert this effect is currently unknown and the subject of further research, the data strongly suggest involvement of VEC modulation at the sites of arthritis involvement. This would indicate the importance of this cell type in the inflammation, and the potential for use of an active VEC-targeting approach for therapeutic intervention in arthritis.

Cell-specific targeting with particulate carriers, and especially liposomes, has long been performed by linkage of rather large targeting ligands, in particular antibodies or antibody fragments, to the liposomal bilayer or, later, to the distal end of the PEG chains of long-circulating liposomes (39–42). More recently, liposomes have been equipped with small peptides for cell-specific targeting (43–46). We show herein that covalent linkage of a cyclic RGD sequence–containing peptide results in specific association of PEG liposomes with HUVECs in vitro, in a liposome dose–, peptide density–, and temperature-dependent manner. Confocal laser scanning microscopy demonstrated that cell binding of the RGD-PEG–L is followed by internalization. Internalization of drug carriers is an attractive feature for intracellular drug delivery. In the case of liposomal DEXP, endocytic uptake and subsequent intracellular processing will yield dexamethasone, the active parent drug. The dexamethasone itself can, by virtue of its amphiphilic nature, easily pass endosomal membranes and reach the glucocorticoid receptor in the cytosol in a manner comparable with that described for a dexamethasone/antibody conjugate (9).

Besides demonstrating in vitro cell binding, we also confirmed in vivo binding of RGD-PEG–L to VECs at inflamed sites in a model of SC LPS–induced inflammation. Our results represent the first demonstration of in vivo targeting of RGD-targeted liposomes to VECs during inflammation. We used a mouse dorsal skin flap window chamber model, which allows examination of liposome–vessel wall interactions in the living animal (37,47). Strong binding of RGD-PEG–L to the vessel wall at the inflamed site was observed 4 hours after induction of inflammation.

The degree of specific targeting of RGD-PEG–L was determined in a rat model of inflammation, also induced by LPS. A 3-fold higher level of localization of RGD-PEG–L at the inflamed site was observed in comparison with localization of RAD-PEG–L or PEG-L, despite the relatively unfavorable circulation kinetics of the RGD-PEG–L (Figure 3). Levels of localization of all 3 types of liposomes in the inflamed skin were higher than those in normal skin. Control

liposomes (RAD-PEG–L or PEG-L) most likely localized in the inflamed skin due to the enhanced permeability and retention effect, as demonstrated for long-circulating liposomes at sites of inflammation or infection (25,48). It has been reported that enhanced permeability and retention–mediated extravasation increases with increasing circulation time of the liposomes (31). Therefore, it is notable that RGD-PEG–L localize to the highest degree at the inflamed site despite their much shorter circulation time. This observation suggests that specific VEC-binding of RGD-PEG–L is more important than enhanced permeability and retention–mediated extravasation.

Treatment of rat AIA with DEXP-containing RGD-PEG–L resulted in stronger antiinflammatory effects compared with DEXP-PEG–L treatment. RGD-DEXP-PEG–L treatment significantly delayed disease development and also resulted in lower arthritis severity throughout the course of the disease. These findings combined with the observation of VEC targeting of RGD-PEG–L to sites of inflammation (demonstrated in this study) as well as to tumor vasculature (38) suggest potentially significant efficacy of RGD-PEG–L–mediated delivery of DEXP to VECs at inflamed sites.

The therapeutic efficacy of free DEXP was not assessed in the present study. However, in previous studies the effects of free corticosteroids such as DEXP and prednisolone phosphate in relation to the efficacy of liposomal formulations have been carefully assessed in this arthritis model as well as in a murine collagen-induced arthritis model. In all of these studies a single administration of free drug exerted minor or no efficacy in alleviating the inflammation, whereas liposomal formulations were efficacious (25–27).

The use of RGD-DEXP-PEG–L allowed early intervention in AIA by targeted delivery of DEXP. Evidence that angiogenesis and related expression of $\alpha v\beta 3$ integrins occur in early phases of AIA has been found in a few studies (49–51). To date, only 2 reports have described the therapeutic potential of RGD-mediated $\alpha v\beta 3$ integrin targeting in arthritis (4,50). Storgard et al intraarticularly injected a cyclic RGD peptide as $\alpha v\beta 3$ integrin antagonist in a rabbit model of AIA (50). Although rapid binding of the peptides to $\alpha v\beta 3$ integrins at the inflamed site 24 hours after disease onset was observed, therapeutic efficacy was obtained only on days 14–28 after disease onset, with weekly repeated intraarticular administration of high doses of peptide (50). Our data, in contrast, reveal immediate therapeutic efficacy resulting from a single IV administration of RGD-DEXP-PEG–L, suggesting that angiogenic processes can be utilized efficiently for drug targeting purposes in arthritis.

Gerlag and colleagues demonstrated considerable efficacy of an IV-administered apoptotic peptide targeted to neovasculature by means of a dicyclic RGD peptide, in the treatment of established collagen-induced arthritis in mice (4). In comparison with the monovalent RGD–apoptotic peptide construct, RGD-PEG–L may well benefit from enhanced affinity for $\alpha v\beta 3$ integrins on angiogenic VECs, since it is a multivalent RGD–exposing system. Multivalent RGD exposure on a protein backbone has been shown to result in enhanced receptor affinity compared with the monovalent free peptide (30).

Corticosteroids have been reported to inhibit expression of several leukocyte adhesion molecules on endothelial cells, thereby reducing leukocyte adherence (17,20–22). Additionally, corticosteroids are known to exert a significant antiangiogenic effect (23,24). Which mechanism is involved in the findings presented here, or whether the two cooperate, is unclear at present, but this will be the subject of further research. Notably, VEC targeting of corticosteroids resulted in a long-lasting disease-suppressive effect, illustrating the promise of this approach for improved therapy in arthritis.

In conclusion, we have developed an RGD-targeted liposomal drug delivery system that specifically binds VECs in vitro and endothelium at sites of inflammation in vivo. Binding resulted in internalization, a prerequisite for efficient intracellular drug delivery. RGD-PEG–L could rapidly target inflammation, as demonstrated by increased RGD-PEG–L localization in LPS-induced inflammation. Using these liposomes to deliver DEXP to VECs at sites of arthritis involvement proved very efficacious in rat AIA, indicating promise for the treatment of rheumatoid arthritis. Future research will focus more precisely on the mechanisms involved and may also explore delivery of other antiinflammatory compounds by the RGD-targeted liposomes.

REFERENCES

1. Griffioen AW, Molema G. Angiogenesis: potentials for pharmacologic intervention in the treatment of cancer, cardiovascular diseases and chronic inflammation. Pharmacol Rev 2000;52: 237–68.
2. Walsh DA, Haywood L. Angiogenesis: a therapeutic target in arthritis. Curr Opin Invest Drugs 2001;2:1054–63.
3. Koning GA, Schiffelers RM, Storm G. Endothelial cells at inflammatory sites as target for therapeutic intervention. Endothelium 2002;9:161–71.
4. Gerlag DM, Borges E, Tak PP, Ellerby HM, Bredesen DE,

Pasqualini R, et al. Suppression of murine collagen-induced arthritis by targeted apoptosis of synovial neovasculature. Arthritis Res 2001;3:357–61.
5. Grosios K, Wood J, Esser R, Raychaudhuri A, Dawson J. Angiogenesis inhibition by the novel VEGF receptor tyrosine kinase inhibitor, PTK787/ZK222584, causes significant anti-arthritic effects in models of rheumatoid arthritis. Inflamm Res 2004;53: 133–42.
6. Goedkoop AY, Kraan MC, Picavet DI, de Rie MA, Teunissen MB, Bos JD, et al. Deactivation of endothelium and reduction in angiogenesis in psoriatic skin and synovium by low dose infliximab therapy in combination with stable methotrexate therapy: a prospective single-centre study. Arthritis Res Ther 2004;6:R326–34.
7. Canete JD, Pablos JL, Sanmarti R, Mallofre C, Marsal S, Maymo J, et al. Antiangiogenic effects of anti–tumor necrosis factor α therapy with infliximab in psoriatic arthritis. Arthritis Rheum 2004;50:1636–41.
8. Muzykantov VR, Christofidou-Solomidou M, Balyasnikova I, Harshaw DW, Schultz L, Fisher AB, et al. Streptavidin facilitates internalization and pulmonary targeting of an anti-endothelial cell antibody (platelet-endothelial cell adhesion molecule 1): a strategy for vascular immunotargeting of drugs. Proc Natl Acad Sci U S A 1999;96:2379–84.
9. Everts M, Kok RJ, Asgeirsdottir SA, Melgert BN, Moolenaar TJ, Koning GA, et al. Selective intracellular delivery of dexamethasone into activated endothelial cells using an E-selectin directed immunoconjugate. J Immunol 2002;168:883–9.
10. Bazzoni G, Dejana E, Lampugnani MG. Endothelial adhesion molecules in the development of the vascular tree: the garden of forking paths. Curr Opin Cell Biol 1999;11:573–81.
11. Eliceiri BP, Cheresh DA. The role of αv integrins during angiogenesis: insights into potential mechanisms of action and clinical development. J Clin Invest 1999;103:1227–30.
12. Koivunen E, Wang B, Ruoslahti E. Phage libraries displaying cyclic peptides with different ring sizes: ligand specificities of the RGD-directed integrins. Biotechnology 1995;13:265–70.
13. Bloemen PG, Henricks PA, van Bloois L, van den Tweel MC, Bloem AC, Nijkamp FP, et al. Adhesion molecules: a new target for immunoliposome-mediated drug delivery. FEBS Lett 1995; 357:140–4.
14. Bendas G, Krause A, Schmidt R, Vogel J, Rothe U. Selectins as new targets for immunoliposome-mediated drug delivery: a potential way of anti-inflammatory therapy. Pharm Acta Helv 1998;73: 19–26.
15. Burke-Gaffney A, Hellewell PG. Regulation of ICAM-1 by dexamethasone in a human vascular endothelial cell line EAhy926. Am J Physiol 1996;270:C552–61.
16. Brostjan C, Anrather J, Csizmadia V, Natarajan G, Winkler H. Glucocorticoids inhibit E-selectin expression by targeting NF-κB and not ATF/c-Jun. J Immunol 1997;158:3836–44.
17. Wheller SK, Perretti M. Dexamethasone inhibits cytokine-induced intercellular adhesion molecule-1 up-regulation on endothelial cell lines. Eur J Pharmacol 1997;331:65–71.
18. Asgeirsdottir SA, Kok RJ, Everts M, Meijer DK, Molema G. Delivery of pharmacologically active dexamethasone into activated endothelial cells by dexamethasone-anti-E-selectin immunoconjugate. Biochem Pharmacol 2003;65:1729–39.
19. Newton R, Hart LA, Stevens DA, Bergmann M, Donnelly LE, Adcock IM, et al. Effect of dexamethasone on interleukin-1β-(IL-1β)-induced nuclear factor-κB (NF-κB) and κB-dependent transcription in epithelial cells. Eur J Biochem 1998;254:81–9.
20. Cronstein BN, Kimmel SC, Levin RI, Martiniuk F, Weissmann G. A mechanism for the antiinflammatory effects of corticosteroids: the glucocorticoid receptor regulates leukocyte adhesion to endothelial cells and expression of endothelial-leukocyte adhesion molecule 1 and intercellular adhesion molecule 1. Proc Natl Acad Sci U S A 1992;89:9991–5.
21. Eguchi K, Kawakami A, Nakashima M, Ida H, Sakito S, Matsuoka N, et al. Interferon-α and dexamethasone inhibit adhesion of T cells to endothelial cells and synovial cells. Clin Exp Immunol 1992;88:448–54.
22. Pitzalis C, Pipitone N, Bajocchi G, Hall M, Goulding N, Lee A, et al. Corticosteroids inhibit lymphocyte binding to endothelium and intercellular adhesion: an additional mechanism for their anti-inflammatory and immunosuppressive effect. J Immunol 1997;158: 5007–16.
23. Hori Y, Hu DE, Yasui K, Smither RL, Gresham GA, Fan TP. Differential effects of angiostatic steroids and dexamethasone on angiogenesis and cytokine levels in rat sponge implants. Br J Pharmacol 1996;118:1584–91.
24. Jackson JR, Seed MP, Kircher CH, Willoughby DA, Winkler JD. The codependence of angiogenesis and chronic inflammation. FASEB J 1997;11:457–65.
25. Metselaar JM, Wauben MH, Wagenaar-Hilbers JP, Boerman OC, Storm G. Complete remission of experimental arthritis by joint targeting of glucocorticoids with long-circulating liposomes. Arthritis Rheum 2003;48:2059–66.
26. Metselaar JM, van den Berg WB, Holthuysen AE, Wauben MH, Storm G, van Lent PL. Liposomal targeting of glucocorticoids to synovial lining cells strongly increases therapeutic benefit in collagen type II arthritis. Ann Rheum Dis 2004;63:348–53.
27. Metselaar JM, Bruin P, de Boer LW, de Vringer T, Snel C, Oussoren C, et al. A novel family of L-amino acid-based biodegradable polymer-lipid conjugates for the development of long-circulating liposomes with effective drug-targeting capacity. Bioconjug Chem 2003;14:1156–64.
28. Allen TM, Hansen C, Martin F, Redemann C, Yau Young A. Liposomes containing synthetic lipid derivatives of poly(ethylene glycol) show prolonged circulation half-lives in vivo. Biochim Biophys Acta 1991;1066:29–36.
29. Dechantsreiter MA, Planker E, Matha B, Lohof E, Holzemann G, Jonczyk A, et al. N-methylated cyclic RGD peptides as highly active and selective α(V)β(3) integrin antagonists. J Med Chem 1999;42:3033–40.
30. Kok RJ, Schraa AJ, Bos EJ, Moorlag HE, Asgeirsdottir SA, Everts M, et al. Preparation and functional evaluation of RGD-modified proteins as α(v)β(3) integrin directed therapeutics. Bioconjug Chem 2002;13:128–35.
31. Schiffelers RM, Bakker-Woudenberg IA, Snijders SV, Storm G. Localization of sterically stabilized liposomes in Klebsiella pneumoniae-infected rat lung tissue: influence of liposome characteristics. Biochim Biophys Acta 1999;1421:329–39.
32. Koning GA, Morselt HW, Velinova MJ, Donga J, Gorter A, Allen TM, et al. Selective transfer of a lipophilic prodrug of 5-fluorodeoxyuridine (FUdR) from immunoliposomes to colon cancer cells. Biochim Biophys Acta 1999;1420:153–67.
33. Bottcher CJ, van Gent CM, Pries C. A rapid and sensitive sub-micro phosphorus determination. Anal Chim Acta 1961;24: 203–4.
34. Bligh EG, Dyer EJ. A rapid method of total lipid extraction and purification. Can J Biochem Physiol 1959;37:911–7.
35. Kirpotin D, Park JW, Hong K, Zalipsky S, Li WL, Carter P, et al. Sterically stabilized anti-HER2 immunoliposomes: design and targeting to human breast cancer cells in vitro. Biochemistry 1997;36:66–75.
36. Jaffe EA, Nachman RL, Becker CG, Minick CR. Culture of human endothelial cells derived from umbilical veins: identification by morphologic and immunologic criteria. J Clin Invest 1973;52:2745–56.
37. Papenfuss HD, Gross JF, Intaglietta M, Treese FA. A transparent access chamber for the rat dorsal skin fold. Microvasc Res 1979;18:311–8.
38. Schiffelers RM, Koning GA, ten Hagen TL, Fens MH, Schraa AJ, Janssen AP, et al. Anti-tumor efficacy of tumor vasculature-

targeted liposomal doxorubicin. J Control Release 2003;91: 115–22.
39. Koning GA, Morselt HW, Gorter A, Allen TM, Zalipsky S, Kamps JA, et al. Pharmacokinetics of differently designed immunoliposome formulations in rats with or without hepatic colon cancer metastases. Pharm Res 2001;18:1291–8.
40. Martin FJ, Hubbell WL, Papahadjopoulos D. Immunospecific targeting of liposomes to cells: a novel and efficient method for covalent attachment of Fab′ fragments via disulfide bonds. Biochemistry 1981;20:4229–38.
41. Mastrobattista E, Koning GA, Storm G. Immunoliposomes for the targeted delivery of antitumor drugs. Adv Drug Deliv Rev 1999; 40:103–27.
42. Everts M, Koning GA, Kok RJ, Asgeirsdottir SA, Vestweber D, Meijer DK, et al. In vitro cellular handling and in vivo targeting of E-selectin-directed immunoconjugates and immunoliposomes used for drug delivery to inflamed endothelium. Pharm Res 2003;20:64–72.
43. Zalipsky S, Puntambekar B, Boulikas P, Engbers CM, Woodle MC. Peptide attachment to extremities of liposomal surface grafted PEG chains: preparation of the long-circulating form of laminin pentapeptide, YIGSR. Bioconjug Chem 1995;6:705–8.
44. Moreira JN, Ishida T, Gaspar R, Allen TM. Use of the post-insertion technique to insert peptide ligands into pre-formed stealth liposomes with retention of binding activity and cytotoxicity. Pharm Res 2002;19:265–9.
45. Jaafari MR, Foldvari M. Targeting of liposomes to melanoma cells with high levels of ICAM-1 expression through adhesive peptides from immunoglobulin domains. J Pharm Sci 2002;91:396–404.
46. Schiffelers RM, Molema G, ten Hagen TL, Janssen AP, Schraa AJ, Kok RJ, et al. Ligand-targeted liposomes directed against pathological vasculature. J Liposome Res 2002;12:129–35.
47. Yuan F, Leunig M, Huang SK, Berk DA, Papahadjopoulos D, Jain RK. Microvascular permeability and interstitial penetration of sterically stabilized (stealth) liposomes in a human tumor xenograft. Cancer Res 1994;54:3352–6.
48. Schiffelers RM, Bakker-Woudenberg IA, Storm G. Localization of sterically stabilized liposomes in experimental rat Klebsiella pneumoniae pneumonia: dependence on circulation kinetics and presence of poly(ethylene)glycol coating. Biochim Biophys Acta 2000; 1468:253–61.
49. Walsh DA, Rodway HA, Claxson A. Vascular turnover during carrageenan synovitis in the rat. Lab Invest 1998;78:1513–21.
50. Storgard CM, Stupack DG, Jonczyk A, Goodman SL, Fox RI, Cheresh DA. Decreased angiogenesis and arthritic disease in rabbits treated with an $\alpha v\beta 3$ antagonist. J Clin Invest 1999;103: 47–54.
51. Kolb C, Mauch S, Krawinkel U, Sedlacek R. Matrix metalloproteinase-19 in capillary endothelial cells: expression in acutely, but not in chronically, inflamed synovium. Exp Cell Res 1999;250: 122–30.